PAPER

Check for updates

Printed dry electrode for neuromuscular electrical stimulation (NMES) for e-textile†

Youssif Merhi, [ID] [a] Pablo F. Betancur, [ID] [b] Teresa S. Ripolles, [ID] [b] Charlotte Suetta,[c] Morten R. Brage-Andersen,[c] Sofie K. Hansen, [ID] [c] Anders Frydenlund,[c] Jens Vinge Nygaard, [ID] [d] Peter H. Mikkelsen,[a] Pablo P. Boix [ID] [b] and Shweta Agarwala [ID] ✱[a]

Muscle atrophy is a well-known consequence of immobilization and critical illness, leading to prolonged rehabilitation and increased mortality. In this study, we develop a solution to preserve muscle mass using customized biocompatible neuromuscular electrical stimulation (NMES) device. Commercially available NMES solutions with gel-based electrodes often lead to skin irritation. We demonstrate the printing of conducting electrodes on a compressive stocking textile that can be used for more than seven days without observing any inflammation. This solution consists of a dry and biocompatible electrode directly integrated into the textile with good mechanical compatibility with skin (Young's modulus of 0.39 MPa). The surface roughness of the underlying substrate plays a significant role in obtaining good print quality. Electrochemical Impedance Spectroscopy (EIS) analysis showed that the printed electrode showed better performance than the commercial ones based on a matched interfacial performance and improved series resistance. Furthermore, we investigated our NMES solution in a hospital setting to evaluate its effective-ness on muscle atrophy, with promising results.

Introduction

The weakness acquired during hospitalization for critical illness is increasingly recognized as an essential clinical problem. Intensive care unit (ICU) acquired weakness (ICUAW) and related acquired neuromuscular dysfunction occurs in a large percentage of critically ill patients, and is associated with increased morbidity and mortality.[1–3] ICUAW is the main factor affecting ICU patients' recovery and quality of life after discharge. Electrostimulation is a therapeutic approach wherein a low-frequency current is introduced through electrodes to stimulate muscles or nerves. Neuromuscular electrical stimulation (NMES)[4] and functional electrical stimulation (FES)[5] are the subareas of electrostimulation that have been recognized as an alternate therapy form to promote movement in critically ill patients and reduce muscle atrophy. Notably, the loss of muscle mass starts early and fast,[6] with the most

significant loss of mass and function occurring during the first two weeks of the ICU stay,[7] with a decrease of 17.7% in the first ten days.[8] Therefore, it seems paramount to counter-act the loss of muscle mass and muscle strength as early as possible.[6] It has been demonstrated that early exercise training in critically ill patients receiving mechanical ventilation is feasible, safe, and beneficial for respiratory and limb muscles.[9] However, severely critically ill patients, often under sedative drugs, cannot collaborate in active exercise or muscle training. Despite this, NMES is not used in ICU settings because the existing solutions demand specialist care and are challenging to incorporate into the current ICU workflow. There is a need to find a ready answer to prevent loss of muscle mass that can be integrated into the existing workflow and infrastructure of the healthcare system. To this end, much research has been done to develop a patch-based plan and e-textiles to stimulate muscles electrically.

On-skin electrodes are an ideal platform for collecting high-quality electrophysiological signals and stimulating the human body.[10,11] Conventional silver–silver chloride (Ag/AgCl) electrodes have many limitations for practical use in a clinical setting. The gel used for Ag/AgCl electrodes has been shown to cause skin inflammation and irritation over long-term use.[12] Metal foils and thin metal films have been investigated as on-skin electrodes, but their rigid nature hinders the signal during motion due to loss of contact.[13] With the rise of flexible electronics, much emphasis has been laid on the softness,

aDepartment of Electrical and Computer Engineering, Aarhus University, Denmark. E-mail: shweta@ece.au.dk
bUniversidad de Valencia, Instituto de Ciencia de Materiales, Spain
cDepartment of Geriatric and Palliative Medicine, Copenhagen University Hospital–Bispebjerg and Frederiksberg Hospital, Copenhagen, Denmark
dDepartment of Biological and Chemical Engineering, Aarhus University, Denmark
†Electronic supplementary information (ESI) available. See DOI: https://doi.org/10.1039/d2nr06008f

stretchability, and breathability of electrodes.[14] Carbon material-based electrodes have started to play a critical role in flexible electronics; however, converting them into well-dispersed inks for direct-write techniques has been challenging.[15] Polymer materials cannot compete with the high conductivity performance of metal counterparts.[16] Much success has been achieved in formulating metallic nanoparticle materials and inks for on-skin electrodes with different morphologies Li *et al.*, studied and compared three other electrodes (wet, semi-dry, and dry) to find an alternative to gel-based electrodes.[17] They pointed out various factors like skin location, skin condition, and contact area that may affect electrode performance. Building on this knowledge base, we use direct-write printing to fabricate dry electrodes for a multi-layered system to stimulate human muscles. This system matches the interfacial properties of current commercial gel-based electrodes with improved series resistance. This improves the overall stimulation performance, potentially minimizing skin irritation side effects, as demonstrated by the pilot study on ICU-admitted patients.

Experimental section

Materials and methods

An anti-embolism compression stocking made of Spandex (elastane), Nylon, and silicone/polyisoprene (strap) manufactured by CAROLYN was purchased from Mediq (Denmark). A Heat transfer buffer layer (B-FLEX BF PRINT00-BF PRINT01) made of PU/Polyurethane was purchased from Vikiallo (Denmark). Thermally curable silver ink (TC-C4007) was purchased from Smart Fabric Inks Ltd (Southampton, UK). All other chemicals were purchased from Sigma Aldrich.

Fabrication and characterization

The textile, an anti-embolism compression stocking made of Spandex, was prepared for a smooth surface for electrodes to be printed on top. This was done using an interface layer. The interface layer was precut using the desktop cutter and laminated on the textile by heat pressing using a Stahls Clam Basic Manual Heat presser (Vikiallo, Denmark). The heat transfer interface layer (B-FLEX BF PRINT00-BF PRINT01) is made from PU/Polyurethane and purchased from Vikiallo (Denmark). The heat and pressure make the interface layer adhere well to the textile. The purchased silver ink (Fabink, TC-C4007) was screen printed without modification on top of the smooth interface layer and processed at 100 °C for 10 minutes in hot air for curing. The dimensions of the printed electrode were 120 mm × 50 mm to enable good coverage of the muscle to be stimulated. The fabrication was completed by adding connectors. The surface morphology of the printed patterns was examined with Scanning Electron Microscopy (SEM) (FEI Magellan 400 SEM). The surface roughness of the samples was analyzed with Atomic Force Microscopy (AFM) (Bruker Dimension Edge). The Root Mean Square was calculated by the equation: $R_q = \sqrt{\dfrac{l}{l_r} \int_0^{l_r} z(x)^2 \mathrm{d}x}$. Contact angle studies were carried out on KRUSS DSA100. Mechanical tests on the samples were carried out on a BOSE ElectroForce® 3220 with a 225 N load cell (±0.002 N) and a displacement sensor (±0.001 mm. The system ran on WinTest7 and DMA software (Bose Corporation, ElectroForce Systems Group, Minnesota, USA). The electrical properties were characterized by a universal four-probe system connected to a Jandel RM3 current generator providing a current range from 1×10^{-8} to 9.9×10^{-2} A. Current density–voltage (J–V) curves and electrochemical impedance spectroscopy (EIS) were measured using a potentiostat/galvanostat Gamry Interface 1010E with a two electrodes system. A commercial electrode, Compex®, with 25 cm^2 of the area, was used as a reference gel electrode. Printed-dry electrode had an area of 5.25 cm^2. The J–V curves were carried out from 0 V to 1.5 V with a 50 mV s^{-1} scan rate. A 20 mV AC perturbation was applied, ranging between 1000 Hz and 0.1 Hz for the impedance spectroscopy measurement at 0.25 V and 0.5 V DC potential steady states. The printed electrodes embedded in the textile were home washed in a Samsung WW95TA047AE washing machine at 60 °C temperature for 30 min at a rate of 1400 RPM. Resistance was measured at five different spots for the cycles, and the average was calculated. All surfaces were scanned in the same areas three times, covering each respective corner and center. Ten printed electrodes of size 1 cm × 3 cm were fabricated for the study.

Pilot study

The clinical pilot study was conducted at Copenhagen University Hospital, Bispebjerg, and Frederiksberg, Copenhagen, Denmark. Within the first 48 hours of admission, seven eligible adults suffering from SARS-CoV-2 (Covid-19) received oral and written information about the study and signed a consent statement before baseline testing. Sonographic scans of the knee extensor muscle thickness (vastus lateralis, VL) were made in the transversal plane of the thigh at 50% femur length. They were defined as half the length from the most proximal point of the greater trochanter of the femur to the tibia plateau. A detailed description of the method for recording ultrasound images has been published elsewhere.[2] However, a modified version of the method was applied in this study. The stocking was worn on one leg while the other leg served as the control. In brief, the thickness of VL was measured by a trained operator with a Doppler Ultrasound system (Sonoscape Medical Coperation) while the patient was lying on a bed with outstretched legs and 120° flexion in the hip. Two images were recorded for each measurement, and each image was later analyzed three times by a blinded observer following a standardized protocol for ultrasound image procedure analysis.[17] Neuromuscular electrical stimulation (NMES) was unilaterally given through our customized anti-embolic compression stocking with built-in electrodes, to a randomized leg (ES), with the opposite leg serving as control (CO). The stimulation protocol was 60 Hz/400 μs, 30 min 2 per day, seven days per week for a minimum of 5 days at a subjective tolerance.

Results and discussion

Conventional fabrication methods to create electrodes suffer require expensive machinery and clean-rooms, high energy usage (vacuum and high temperature systems) and lead to large material wastage. Direct-write techniques provide a complementary platform to enable flexible, stretchable, and conformable electronics. The cost saving in printing technologies comes from 2 main factors, namely (1) saving of materials and (2) systems using low-energy. Screen printing is a room-temperature process that requires very simple equipment and is much cheaper than vacuum deposition techniques. Moreover, the functional inks are used in small quantities (20 ml or so) and deposited when needed, which keeps the cost of fabrication low. Different types of printing techniques have been proposed. Here, Foo, C. Y *et al.*, proposed a novel printable graphene-based conductive filament to create a range of 3D printed electrodes (3DEs) using a commercial 3D printer.[18] This approach provides material fabrication for various applications because of its ability to create low-cost 3D printed platforms. However, 3D printing is not without limitations. Here, one of the main limitations of 3D printing is its slow printing speed and difficult scalability. On the other hand, Screen printing technology is one of the most popular methods of fabricating electrodes on flexible substrates. Benefiting from a relatively simple procedure, the feasibility of mass production, unlike other printing techniques such as 3D printing, changeable patterns, and low cost. Like the traditional method of fabricating electrodes, screen printing technology follows top-down approaches.[19,20] Silver ink is the material of choice due to low resistivity, chemical inertness, and easy processing *via* printed electronics.[21] Screen printing was used to print the silver electrode material on the interfacial layer (Fig. 1A). Optimization of ink viscosity and printing speed was carried out to print conducting electrodes. This resulted in a smooth, dry electrode on the textile. The printed electrode was crack-free, homogeneous, and flexible (Fig. 1B). The silver ink adheres strongly to the substrate through the interface layer over the textile, as depicted in Fig. 1C. The printed electrodes can withstand bending, twisting, and stretching without loss of electrical performance (Fig. 1D).

Surface properties like surface energy, surface tension, and surface roughness of a substrate are primely important in direct-write techniques.[22,23] The SEM micrographs in Fig. 2A depict a highly intricate mesh of fibers in the stocking fabric. Macro-sized voids and pores can be observed in the textile. This surface morphology is not ideal for printing silver ink. Materials with high surface roughness can hinder substrate-ink adhesion and affect the electron transport properties in the electrode. After printing, solvent evaporation, and sintering, mechanical interlocking allows for the nanoparticles in ink to anchor to the substrate. Strong adhesion is thus enabled to provide good performance under different bending, flexing, and stretching conditions. Apart from surface roughness, the combination of the pore size of the substrate and particle size in ink can also undermine the adhesive strength of the ink on the textile. The interface layer reduces the surface roughness and helps to fill up the voids. The surface morphology of the interface layer enables the trapping of the nanoparticles in the ink onto the surface, resulting in better adhesion and good-resolution printing.[24] The cross-sectional image of the printed electrode on the interface layer and the textile is shown in Fig. 2B. The observed thickness of the interfacial layer and printed silver inks was approximately 100 μm
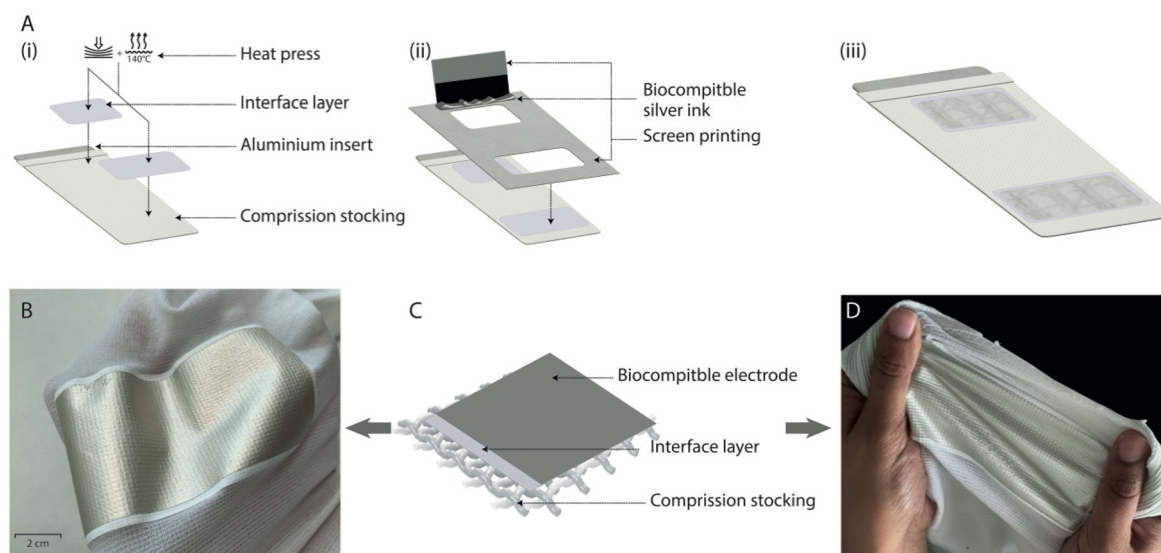

Fig. 1 (A) Schematic of the fabrication process of the e-textile: (i) laying of the interface layer and heat pressing it for adhesion, (ii) screen-printing of silver ink to form the electrode using a stencil and (iii) the final printed e-textile. (B) Picture of the printed silver electrode. The inset shows the zoomed-in image of the electrode. (C) Schematic depicting the coverage of printed silver on a fibrous textile. (D) Picture showing the stretched electrode.
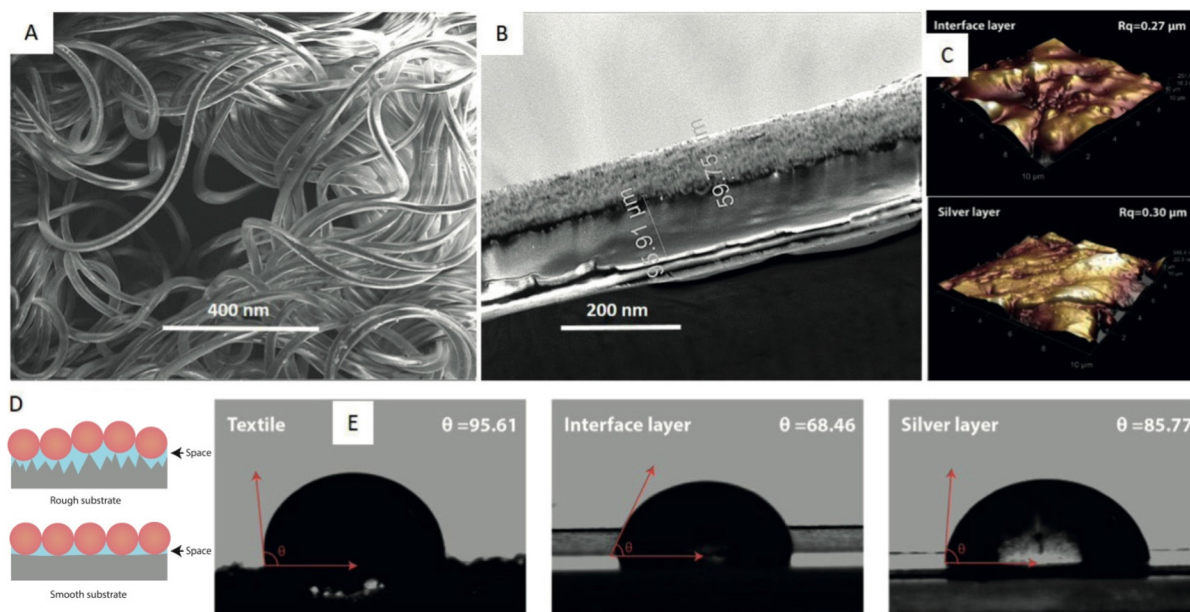
Fig. 2 SEM micrograph depicting (A) the top view of the compression stocking textile and (B) cross-section of the printed electrode on top of the interface layer. (C) AFM images showing the surface roughness of the interface layer and screen-printed silver electrode. (D) Pictorial representation of how surface properties and roughness play a part in achieving good print quality. (E) Water contact angle measured on bare textile, interface layer, and printed silver electrode.

and 60 μm, respectively. Surface roughness strongly affects the contact angle and wettability of a surface and is crucial for preparing surfaces for printed electronics.[25] AFM measurements showed the roughness (R_q) for the textile to be very high (>150 μm), as evident from the SEM micrograph (Fig. 2a). R_q value for the interface layer and printed dry electrode was calculated to be 0.27 μm and 0.30 μm, respectively (Fig. 2C). Thus, it is evident that the interface layer provides a smooth base to print a homogeneous electrode, as depicted in the schematic of Fig. 2D. For repeatability the AFM measurements were conducted on different printed electrodes (Table S1†) and each electrode was measured at five different points to reduce the error (Fig. S1†). The contact angle measurement shows that the textile surface is hydrophobic (Fig. 2E). The interface layer enhances the hydrophilic nature of the textile and prepares it for better wettability for the silver ink. Printed silver electrodes lead to a rough surface but maintain a hydrophilic nature. This makes the dry electrodes suitable for printing if a top layer is needed.

Mechanical tests were performed on the individual printed stocking constituents, *i.e.*, textile, electrode and interface layers to evaluate their elastic and viscoelastic properties. Hysteresis measurements (Fig. 3A) illustrate how elastic energy is deposited into the materials during stretching and recovered during unloading. The area enclosed by the curve expresses the amount of energy permanently deposited into the material leading to a temperature increase.[26] A significant hysteresis loss is seen in the electrode along with complete elastic recovery in the textile. Fig. 3B shows the tensile relaxation measurements revealing the time required for the materials to reach stress equilibrium post an instantaneous load. All three materials show relaxation over

similar time scale at about 0.8 s. Work curves from tensile tests reveal their stiffnesses as the slope of the curves (Fig. 3C). This demonstrates that the electrode material shows the highest stiffness and the textile the lowest. The interface stiffness is selected and shown to be intermediate. This facilitates a structural graduation across the layers and ensure compatibility and improved interlayer adhesion properties when the combined lamina is stretched. To further test the durability and washability of our device, multiple washing cycles were carried out for the fabricated e-textile. A total of 5 washing cycle was done at 40 °C for 30 min and change in resistance was observed. As can be seen from Fig. 3D, a clear trend was observed. Here, the resistance increased with each wash, making the device electrically non-functional after some washes.

As the fabricated electrodes are to be used on the skin, it requires an understanding of the electrode-skin interface and related properties. Fig. 4a shows the *J–V* curves for the printed electrodes compared to a commercially available gel-based reference (Compex®). All the results have been normalized to exclude the effect of electrode surface area. The current intensity measured shows a strong correlation with the position of the electrodes in the subject, with negligible variations regarding small variations of the distance between the electrodes (Fig. 4a). Similarly, the analyzed trend between the samples was reproduced regardless of the subject (Fig. 4b). This behavior indicates that the information obtained by the electrical characterization corresponds mainly to the skin-electrode interface. For all the subjects, the current measured by the printed electrode displays slightly higher values than the commercial electrode, indicating better signal transmission at
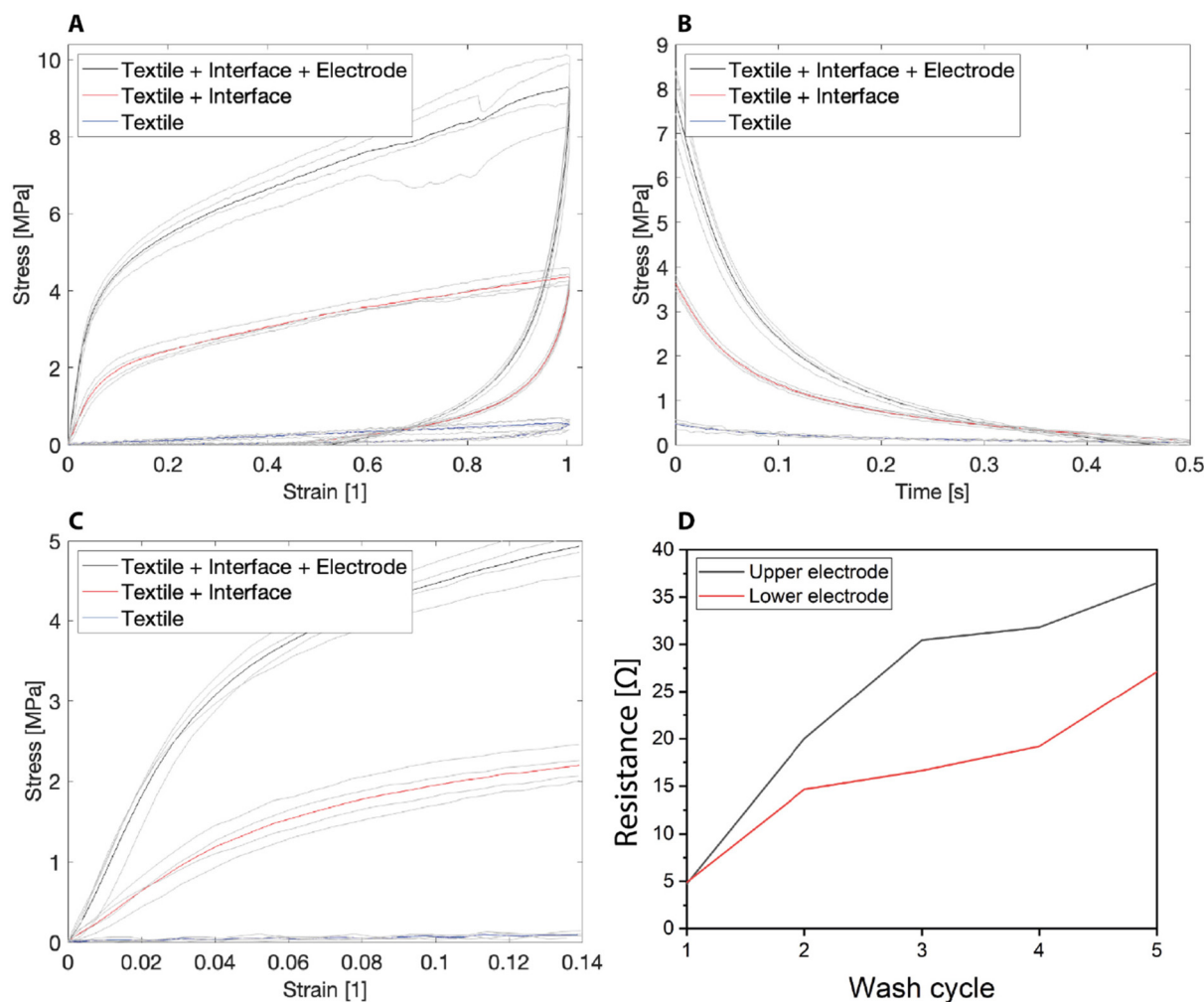
Fig. 3 Mechanical properties of the printed dry electrodes on the textile: (A) Hysteresis measurements, (B) Tensile relaxation measurements and (C) Work curves from tensile tests revealing the stiffness of individual constituents' textile, interface and electrode layers. (D) Measurements of the resistance changes due to washing.

similar conditions (Fig. S2†). To gain further understanding on the electrical properties, electrochemical impedance spectroscopy (EIS) was performed at the electrode-skin interface in a two-contact symmetric configuration (electrode-skin-electrode). EIS has proven to be a great tool for printed electronics and related application and has the power to elucidate design parameters and selection of materials.[27] This frequency-based technique is particularly suitable to study these systems, as it can be applied to different operational conditions. The resulting spectra obtained at 0.5 V and 0.25 V are plotted in Fig. 4b. These Nyquist plots feature one main arc, which suggests that the charge conduction is dominated by one process in both electrodes, attributed to the interface skin/electrode. The trends of these arcs reproduce the JV results, indicating slightly higher resistances for the commercial electrode. The capacitance Bode plots of these spectra (Fig. 4c), can provide further insight on these differences. At higher frequencies, up to 10^4 Hz, the printed dry electrode presents higher capacitance, while the values for both samples are similar under

10^4 Hz. This behavior is related to a variation in the series resistance, R_s, for which evaluation requires a detailed fitting of the results. The equivalent circuit model used to fit the EIS is represented in the ESI (Fig. S1†). In particular, the R_s is in series to the pair interfacial resistance R and interfacial capacitance C which are in parallel. The fitted parameters are represented in Fig. S2.† Interestingly, R and C do not present a significant difference between the samples, corroborating the comparable electrical response at the interface of both printed and commercial electrodes. In contrast, R_s for the printed silver ink devices is around one order of magnitude lower than the commercial one, indicating a reduction in the current losses related to the elimination of an external resistance associated with the gel used in the commercial electrode. This is in good agreement with the capacitance differences and improved signal transmission for the printed dry electrode.

Electrostimulation can be applied to various body parts to prevent or reduce muscle atrophy. For this work, the dry electrode system was used on the thigh (Vastus lateralis, VL)
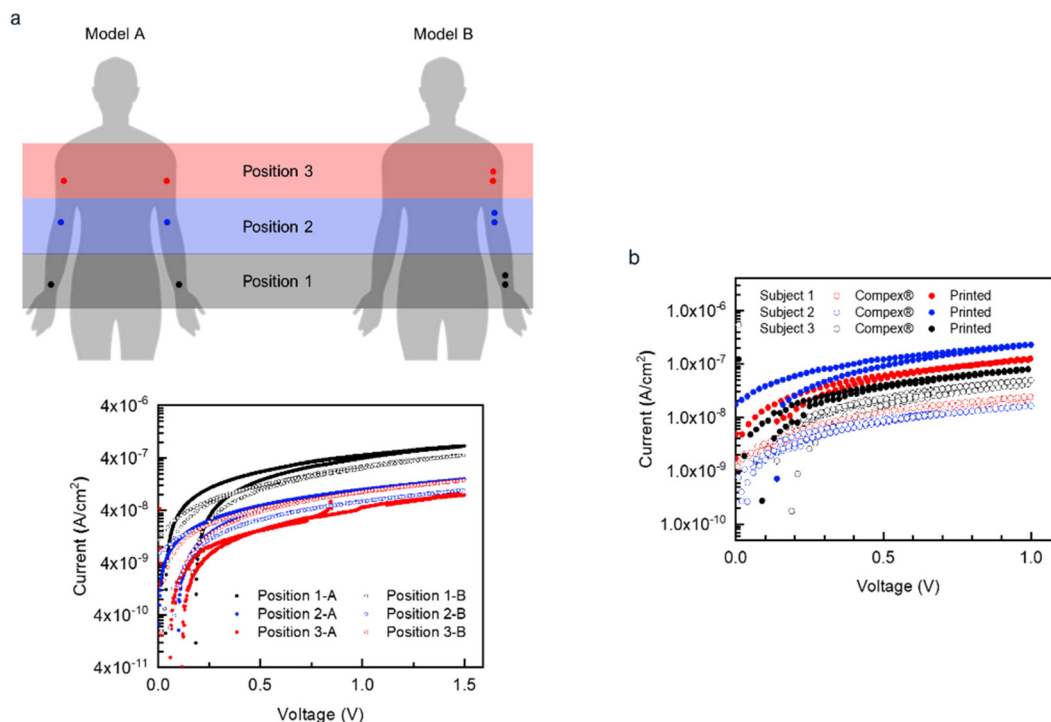
Fig. 4 (a) Schematics of the JV and EIS measurement conditions. In model condition A the electrodes were placed in the same body zone, mirroring one another. In model condition B, the electrodes were placed in the same arm at 3 cm distance between them. The JV curve shows that the location of the electrodes plays a dominant role in the signal measured compared to the physical distance between them, with position 1 being optimal. (b) JV curves for three subjects show a relatively small variation between tested people, with consistently higher currents for the printed dry electrode.

muscles to be stimulated.[2] The printed electrode dimensions were chosen to allow good coverage of the Vastus lateralis muscle. The fabricated customized anti-embolic stocking with the printed electrode was used as the NMES treatment on a small group of patients on a randomized leg (ES), with the opposite leg serving as control (CO) (Fig. 5A). In this pilot study, seven men (55 ± 22 years; height: 179.5 ± 7.0; weight: 102.3 ± 27.8 kg; BMI: 31.5 ± 6.8 kg m^{-2}) completed five days of treat-
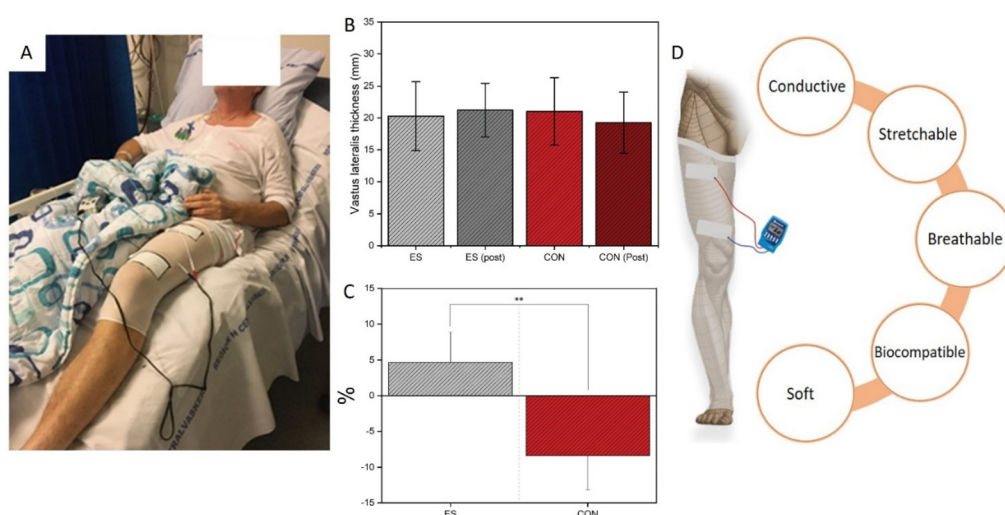

Fig. 5 (A) Photograph of the dry electrode e-textile system for thigh muscles on a patient admitted to the intensive care unit (ICU). Data for seven patients with COVID-19 before and after five days of electric stimulation (ES) of muscle on one leg. The stocking was worn on one leg while the other leg received no stimulation and served as the control (CON). Change in the muscle vastus lateralis (B) thickness and (C) % change in muscle strength. (D) Schematic illustrating the features of the printed dry electrode system on an anti-embolic stocking for a customizable NMES solution.

ment with no complications or skin reactions. It is to be noted that the e-textile with the electrodes was worn during the entire hospital stay. The paired t-test analysis revealed a significant decrease in vastus lateralis thickness from pre to post in the CON-leg (21.0 mm ± 5.3 $vs.$ 19.2 mm ± 4.8 (mean ± SD) respectfully, p = 0.001; compared with no significant change in the ES-leg from pre to post (20.3 mm ± 5.4 $vs.$ 21.2 mm ± 4.2 (mean ± SD) respectfully, p = 0.55 (Fig. 5B). In addition, the unpaired nonparametric analysis (Mann–Whitney) showed a significant group difference for the relative change in VL thickness between the ES-leg and the CON-leg (+4.7% $vs.$ −8.4%, respectively, p = 0.008). The clinical data demonstrated that muscle wasting was counteracted on the treated compared to the untreated leg in severely ill COVID-19 patients. Five days of treatment-maintained muscle mass compared to a −8.4% muscle loss in the control leg (Fig. 5C). Our clinical trial has shown that our method is successful in avoiding muscle loss and thus renders it likely that our system will reduce the number of patients acquiring Intensive care unit-acquired weakness (ICUAW). The customized anti-embolic stocking is feasible in an ICU setting. It may be a promising solution to counteract further muscle wasting in critically ill patients as it encompasses desirable stretchability, breathability, and biocompatibility while eliminating the need to use gels for better skin contact (Fig. 5D).

Conclusions

We developed a customizable NMES treatment solution using a printed electronics technique in this work. Biocompatible silver ink was used to print a dry-electrode system on an anti-embolic stocking, providing electrical stimulation to the thigh (Vastus lateralis) muscles. Screen printing enabled homogeneous and flexible electrodes on the textile with good adhesion. Impedance studies at the skin-electrode interface revealed that the printed dry electrode has better signal transmission than commercial gel-based electrodes. The fabricated system was used for a pilot study for NMES treatment on a small group of patients in the ICU. Five days of treatment-maintained muscle mass compared to a −8.4% muscle loss in the control leg. This signifies the feasibility of using the fabricated system as a promising solution to counteract muscle wasting in critically ill patients in hospital settings.

Author contributions

S. Agarwala, C. Suetta, J. V. Nygaard, P. H. Mikkelsen conceptualized the idea. Y. Merhi carried out the research pertaining to printing, characterization, and device fabrication. P. F. Betancur, T. S. Ripolles, P. P. Boix carried out the EIS measurements. M. R. Brage-Andersen, S. K. Hansen, A. Frydenlund, C. Suetta carried out the pilot study in a hospital setting. S. Agarwala, C. Suetta, J. V. Nygaard, P. H. Mikkelsen, Y. Merhi, P. P. Boix were involved in writing, reviewing, and editing the manuscript.

Conflicts of interest

The authors declare no conflict of interest.

Acknowledgements

References

1 G. Hermans and G. Van den Berghe, Clinical review: intensive care unit acquired weakness, $Crit.$ $Care$, 2015, **19**(1), 274.

2 A. Frydenlund, et $al.$, Electrical stimulation against loss of muscles and function in a patient admitted with COVID-1, $Ugeskr.$ $Laeg.$, 2021, **183**(20), V03210275.

3 H. Lad, et $al.$, Intensive Care Unit-Acquired Weakness: Not just Another Muscle Atrophying Condition, $Int.$ $J.$ $Mol.$ $Sci.$, 2020, **21**(21), 7840.

4 B. M. Doucet, A. Lam and L. Griffin, Neuromuscular electrical stimulation for skeletal muscle function, $Yale$ $J.$ $Biol.$ $Med.$, 2012, **85**(2), 201–215.

5 C. Couppé, et $al.$, The effects of immobilization on the mechanical properties of the patellar tendon in younger and older men, $Clin.$ $Biomech.$, 2012, **27**(9), 949–954.

6 W. Gruther, et $al.$, Muscle wasting in intensive care patients: ultrasound observation of the M. quadriceps femoris muscle layer, $J.$ $Rehabil.$ $Med.$, 2008, **40**(3), 185–189.

7 Z. A. Puthucheary, et $al.$, Acute skeletal muscle wasting in critical illness, $J.$ $Am.$ $Med.$ $Assoc.$, 2013, **310**(15), 1591–1600.

8 C. Burtin, et $al.$, Early exercise in critically ill patients enhances short-term functional recovery, $Crit.$ $Care$ $Med.$, 2009, **37**(9), 2499–2505.

9 H. Wu, et $al.$, Materials, Devices, and Systems of On-Skin Electrodes for Electrophysiological Monitoring and Human-Machine Interfaces, $Adv.$ $Sci.$, 2021, **8**(2), 2001938.

10 H. Kim, et $al.$, Advances in Soft and Dry Electrodes for Wearable Health Monitoring Devices, $Micromachines$, 2022, **13**(4), 629.

11 V. T. Krasteva and S. P. Papazov, Estimation of current density distribution under electrodes for external defibrillation, $Biomed.$ $Eng.$ $Online$, 2002, **1**(1), 7.

12 Z. Zhao, et $al.$, Nanoelectronic Coating Enabled Versatile Multifunctional Neural Probes, $Nano$ $Lett.$, 2017, **17**(8), 4588–4595.

13 S. Huang, et $al.$, Flexible Electronics: Stretchable Electrodes and Their Future, $Adv.$ $Funct.$ $Mater.$, 2019, **29**(6), 1805924.

14 L. Zhuo, On-skin graphene electrodes for large area electrophysiological monitoring and human-machine interfaces, $Carbon$, 2020, **164**, 164–170.

15 F. Stauffer, *et al.*, Skin Conformal Polymer Electrodes for Clinical ECG and EEG Recordings, *Adv. Healthcare Mater.*, 2018, **7**(7), 1700994.

16 G. Li, S. Wang and Y. Y. Duan, Towards gel-free electrodes: A systematic study of electrode-skin impedance, *Sens. Actuators, B*, 2017, **241**, 1244–1255.

17 J. Vahlgren, *et al.*, Using ultrasonography to detect loss of muscle mass in the hospitalized geriatric population, *Transl. Sports Med.*, 2019, **2**(5), 287–293.

18 C. Y. Foo, *et al.*, Three-Dimensional Printed Electrode and Its Novel Applications in Electronic Devices, *Sci. Rep.*, 2018, **8**(1), 7399.

19 Q. Li, *et al.*, Review of Printed Electrodes for Flexible Devices, *Front. Magn. Mater.*, 2019, **5**, DOI: **10.3389/fmats.2018.00077**.

20 K. Yang, *et al.*, Screen printed fabric electrode array for wearable functional electrical stimulation, *Sens. Actuators, A*, 2014, **213**, 108–115.

21 Y. Li, Y. Wu and B. S. Ong, Facile Synthesis of Silver Nanoparticles Useful for Fabrication of High-Conductivity Elements for Printed Electronics, *J. Am. Chem. Soc.*, 2005, **127**(10), 3266–3267.

22 J. Wiklund, *et al.*, A Review on Printed Electronics: Fabrication Methods, Inks, Substrates, Applications and Environmental Impacts, *J. Manuf. Mater. Process.*, 2021, **5**(3), 89.

23 M. M. Hasan and M. M. Hossain, Nanomaterials-patterned flexible electrodes for wearable health monitoring: a review, *J. Mater. Sci.*, 2021, **56**(27), 14900–14942.

24 V. Beedasy and P. J. Smith, Printed Electronics as Prepared by Inkjet Printing, *Materials*, 2020, **13**(3), 704.

25 K. Kubiak, *et al.*, Wettability versus roughness of engineering surfaces, *Wear*, 2011, **271**, 523–528.

26 A. Blonder and M. Brocato, Layered-Fabric Materiality Fibre Reinforced Polymers (L-FMFRP): Hysteretic Behavior in Architectured FRP Material, *Polymers*, 2022, **14**(6), 1141.

27 G. L. Goh, *et al.*, Potential of Printed Electrodes for Electrochemical Impedance Spectroscopy (EIS): Toward Membrane Fouling Detection, *Adv. Bioelectron. Mater.*, 2021, **7**(10), 2100043.